Condensation of a vapor bubble in sub-micrometer container

V. Babin

Institute of Physical Chemistry, Polish Academy of Sciences

Kasprzaka 44/52, 01-224 Warsaw, Poland

R. Hołyst

Institute of Physical Chemistry, Polish Academy of Sciences

Kasprzaka 44/52, 01-224 Warsaw, Poland and

Dept. of Mathematics and Natural Science,

Cardinal Stefan Wyszyński University

Dewajtis 5, 01-815 Warsaw, Poland

(Dated: May 20, 2005)

Abstract

Condensation of a spherically symmetric sub-micrometer size vapor bubble is studied using diffuse interface hydrodynamic model supplemented by the van der Waals equation of state with parameters characteristic for argon. The bubble, surrounded by liquid, is held in a container with temperature of the walls kept fixed. The condensation is triggered by a sudden rise of the walls temperature. We find that the process is totally different from the evaporation. In particular, the rapid change of the walls temperature excites the wave, which hits the interface and compresses the bubble, leading to a considerable increase of the temperature inside. The condensation of the sub-micrometer size bubble takes tens of nanoseconds, whereas evaporation of the same size droplet lasts roughly fifty times longer. In contrast to evaporation the condensation process is hardly quasi-stationary.

I. INTRODUCTION

Evaporation/condensation processes attract much attention because they are ubiquitous in nature and technological applications. Despite the large progress made since the end of XIX century, the phenomena has not been studied in detail in mesoscale [1]. Recently we have undertaken a task of describing the evaporation process of thin films and small droplets in sub-micrometer size containers [2, 3]. We found that the evaporation process proceeds practically quasi-stationary with the temperature and chemical potential both being continuous at the liquid/vapor interface. Under these assumptions the time dependence of the radius of the evaporating droplet can be determined using the energy balance at the interface [3]:

$$R^2(t) = R^2\big|_{t=0} - t\frac{2\kappa_v}{\ell n_l}\left(T_w - T_l\right),$$

where n_l and T_l are the density and temperature of liquid inside the droplet, respectively; κ_v is the heat conductivity of the vapor at the temperature $T = T_l$; ℓ is the latent heat of transition per molecule at $T = T_l$; and T_w is the temperature of the container walls (just to get some feeling: the time required for complete evaporation of argon droplet of radius 669Å is $\approx 1.45\mu$s for $T_l = 128$K and $T_w = 143.2$K). We have compared the time dependence of the droplet radius predicted by the above simple formula with the results of molecular dynamics simulation of evaporation of the droplet consisting of fifty thousands argon atoms [4] with $T_w = 300K$, $T_l = 138K$, and, surprisingly enough, have found rather good agreement.

It is the purpose of this paper to describe the condensation of a small vapor bubble in a sub-micrometer container. We are unaware of any previous study of condensation of a micrometer or sub-micrometer bubbles, where the profiles of various thermodynamic quantities are shown in the course of condensation. It is also unclear how the radius of such

bubbles changes in the course of time. One may reasonably expect that the condensation process is much different from evaporation since there are large difference in compressibility and heat conductivity between vapor and liquid phases; moreover, when the vapor condenses the heat is released which disturbs the condensation process.

Dynamics of the flows accompanied by condensation/evaporation processes is usually modeled in sharp interface approximation [5]. In this approach the interface separating liquid/vapor domains is assumed to be infinitely thin and equations of classical hydrodynamics are used to describe the motion of each phase separately. The phase transition is captured by setting the appropriate boundary conditions at the interface. Different boundary conditions are employed in the literature. Some authors (see, e.g., Refs. [6, 7]) assume continuity of the temperature across the interface. There is, however, theoretical [8] and experimental [9] evidence that the temperature may be discontinuous. Another important issue concerns the mass flux across the interface. Often the Hertz–Knudsen formula is employed in this place. It is obtained under the assumption that the mean free path of molecules in the vapor phase is much larger than the interfacial width [10]. This assumption may not hold if the vapor phase is dense, and different boundary conditions have to be imposed, e.g., the continuity of chemical potential [11, 12].

Here we pose the following questions: Is there any difference between evaporation of droplets and condensation of bubbles? Can we describe the condensation of vapor bubbles in some quasi-stationary approximation? Not too far from the liquid/vapor critical point these questions can be addressed efficiently with the use of appropriately combined diffuse-interface theory and hydrodynamics [13–16]. In this approach the interfacial region is represented by continuous variations of density in a way consistent with microscopic theories of the interface [17]. The need of the interfacial boundary conditions is thus eliminated.

The paper is organized as follows: in the next section we briefly describe the model; in section III we present numerical results and comment them a little; last section contains the summary.

II. THE MODEL

We use diffuse interface model coupled with hydrodynamic equations [14–16, 18]. The set of dynamical equations [15] comprises conservation of mass:

$$\partial_t \rho + \partial_\alpha \left(\rho u_\alpha\right) = 0, \tag{1}$$

conservation of momentum:

$$\partial_t \left(\rho u_\alpha\right) + \partial_\beta \Big(\rho u_\alpha u_\beta + p\delta_{\alpha\beta} - K\sigma^{(c)}_{\alpha\beta}\Big) = \partial_\beta \sigma^{(v)}_{\alpha\beta}, \tag{2}$$

and, equation for the entropy density:

$$T\Big\{\partial_t \left(\rho s\right) + \partial_\alpha \left(u_\alpha \rho s\right)\Big\} = \sigma^{(v)}_{\alpha\beta}\partial_\alpha u_\beta - \partial_\alpha q_\alpha, \tag{3}$$

where ρ is the medium mass density, u_α is the velocity, s is the specific entropy (entropy per unit mass), T is the temperature, p is the thermodynamic pressure, and K is the constant related to the liquid–vapor surface tension. Greek indices label vector and tensor components in Cartesian coordinates and the familiar summation convention: $a_\alpha b_\alpha = a_x b_x + a_y b_y + a_z b_z$ is understood. ∂_α stands for $\partial/\partial x_\alpha$ and ∂_t denotes partial derivative with respect to the time t.

The viscous stress tensor $\sigma^{(v)}_{\alpha\beta}$ has the Newtonian form [19] with bulk viscosity set to zero

$$\sigma^{(v)}_{\alpha\beta} = \rho\nu\Big(\partial_\alpha u_\beta + \partial_\beta u_\alpha - \frac{2}{3}\delta_{\alpha\beta}\partial_\gamma u_\gamma\Big).$$

The heat flux q_α is given by the Fourier Law

$$q_\alpha = -\kappa\partial_\alpha T,\ \kappa = c_v n \chi. \tag{4}$$

Here c_v is the specific heat for constant volume, n is the particle density (i.e., $\rho = mn$, where m is the particle mass). Kinematic viscosity ν as well as thermal diffusivity χ [1], are assumed constant.

Momentum equation (2) coincides with the classical Navier–Stokes equation except of the capillary stress tensor

$$\sigma^{(c)}_{\alpha\beta} = \Big(n\nabla^2 n + \frac{1}{2}\,|\nabla n|^2\Big)\delta_{\alpha\beta} - \partial_\alpha n\;\partial_\beta n, \tag{5}$$

which models capillary forces associated with the interface.

For more detailed description of the model interested reader is referred to the excellent works [15, 16, 20, 21].

A. Dimensionless form

The variables are set to non-dimensional form by means of the length δ_L, energy δ_E temperature δ_T and time δ_t scales obtained from the critical density n_c (that is, particle density at the critical point), critical temperature T_c and molecular mass m of the substance:

$$\delta_L = n_c^{-1/3},\ \delta_E = k_B T_c,\ \delta_T = T_c,\ \delta_t^2 = \frac{m\delta_L^2}{\delta_E}, \tag{6}$$

where k_B is the Boltzmann constant. Dimensionless quantities (marked with tildes) can be then related to the physical ones

$$\begin{aligned}
&x_\alpha = \delta_L \widetilde{x}_\alpha,\ t = \delta_t \widetilde{t},\ \rho = \frac{m}{\delta_L^3}\widetilde{n},\ n = \frac{1}{\delta_L^3}\widetilde{n},\\
&u_\alpha = \frac{\delta_L}{\delta_t}\widetilde{u}_\alpha,\ T = \frac{1}{T_c}\widetilde{T},\ p = \frac{\delta_E}{\delta_L^3}\widetilde{p},\ s = \frac{\delta_E}{T_c m}\widetilde{s},\\
&\widetilde{K} = \frac{1}{\delta_E \delta_L^5}K,\ \widetilde{\nu} = \frac{\delta_t}{\delta_L^2}\nu,\ \widetilde{c_v} = \frac{1}{k_B}c_v,\ \widetilde{\chi} = \frac{\delta_t}{\delta_L^2}\chi.
\end{aligned}$$

[1] Strictly speaking, thermal diffusivity (or thermotropic conductivity) is defined in Ref. [19] using the specific heat at constant pressure $\chi = \kappa/nc_p$.

In non-dimensional form Eqs. (1) - (3) remain unaltered except of the mass density ρ, which is substituted by the dimensionless particle density $\widetilde{n}$. Henceforth we omit the tildes and always use dimensionless quantities unless stated otherwise.

B. Equations of state

The system of equations (1) - (3) is supplemented with two equations of state: $p = p(n, T)$ and $s = s(n, T)$, which can be obtained from the bulk free energy density $f(n, T)$. We use approximate van der Waals formula, which, for noble gases, reads [22]

$$f(n,T) = nT \ln \frac{n}{3-n} - nT - \frac{9}{8}n^2 - \frac{3}{2}nT \ln \lambda T, \tag{7}$$

where

$$\lambda = \left(\frac{1}{3n_c}\right)^{2/3} \frac{mk_B T_c}{2\pi\hbar^2}.$$

In the last expression, n_c and T_c are the dimensional critical density and temperature respectively, and $\hbar$ is the Planck constant.

From (7) we have the pressure

$$p = -f + n\left(\frac{\partial f}{\partial n}\right)_T = \frac{3nT}{3-n} - \frac{9}{8}n^2, \tag{8}$$

the entropy density

$$sn = -\left(\frac{\partial f}{\partial T}\right)_n = \frac{5}{2}n + \frac{3}{2}n \ln \lambda T - n \ln \frac{n}{3-n}, \tag{9}$$

and the specific heat per molecule at constant volume: $c_v = 3/2$.

For temperature $T = 1 - \delta T$, $\delta T > 0$ below $T_c = 1$, the formula (7) predicts coexistence of liquid and vapor phases [22]; their densities n_l and n_v can be determined from the requirement of equal pressures and chemical potentials in the two phases (see Fig.1).

Surface tension of the stationary planar liquid–vapor interface is then given by the following expression [17]

$$\sigma = \sqrt{2K} \int_{n_v}^{n_l} \mathrm{d}n \sqrt{f(n) - \mu_{eq} n + p_{eq}}, \tag{10}$$

where μ_{eq} and p_{eq} are equilibrium values of the chemical potential and pressure correspondingly. For not too large δT the integral in the above formula can be evaluated to give

$$\sigma \approx \sqrt{2K}\,(\delta T)^{3/2} \left[4 - \frac{82}{125}\delta T - \frac{5533}{61250}\,(\delta T)^2 \right] .$$

We have found this approximation to be sufficiently accurate for $\delta T \lesssim 0.4$.

To make a connection with the experiment we have chosen the material constants corresponding to argon. Physical properties of argon are freely available from the NIST web site [23]. In particular, critical density and critical temperature of argon are

$$n_c = 13407.4 \frac{\mathrm{mol}}{\mathrm{m}^3},\ T_c = 150.687\mathrm{K},$$

which gives

$$\delta_L = 4.99 \times 10^{-10} m,\ \delta_t = 2.82 \times 10^{-12} s,\ \lambda = 235.9.$$

The remaining parameters can be approximated by the following constant values:

$$K = 1.3,\ \nu \approx 1,\ \chi \approx 2.$$

We note that the surface tension of the liquid–vapor interface given by Eq.(10) agrees quite well with that of argon in wide range of temperatures (from $T \sim 0.6$ up to the narrow critical region near $T_c = 1$, in dimensionless units). On the other hand, neither kinematic viscosity ν nor thermal diffusivity χ of argon are constants. The values chosen provide tolerable approximation in the range of temperatures relevant to our study $0.8 \lesssim T \lesssim 1$.

C. Spherically symmetric case

We consider a vapor bubble and liquid in a container with the temperature of the walls of container, T_w, kept fixed. Initially the system is in thermodynamic equilibrium. The condensation is triggered by a sudden increase of T_w. We assume that the system is spherically symmetric and, moreover, that the resulting flow is also spherically symmetric, that is,

$$n = n(r,t),\ s = s(r,t),\ u_\alpha = u(r,t)x_\alpha/r,$$

where $r^2 = x_\alpha x_\alpha$ is the distance measured from the center of the bubble, and $\partial_r = \partial/\partial r$. In spherical coordinates the dimensionless equations of motion (1) – (3) reduce to:

$$\partial_t n + \frac{1}{r^2}\partial_r\left(r^2 n u\right) = 0, \tag{11}$$

$$\begin{aligned}\partial_t\left(nu\right) \ + \ \partial_r\left[nu^2 + p - K\left(n\left\{\partial_r^2 n + \frac{2}{r}\partial_r n\right\} - \frac{1}{2}\left(\partial_r n\right)^2\right) - \frac{4}{3}\eta\left(\partial_r u - \frac{1}{r}u\right)\right] = \\ - \ \frac{2}{r}K\left(\partial_r n\right)^2 + \frac{4}{r}\eta\left(\partial_r u - \frac{1}{r}u\right),\end{aligned} \tag{12}$$

$$\partial_t\left(ns\right) + \frac{1}{r^2}\partial_r\left(r^2\left[nsu - \kappa\frac{\partial_r T}{T}\right]\right) = \frac{4}{3}\frac{\eta}{T}\left(\partial_r u - \frac{u}{r}\right)^2 + \kappa\left(\frac{\partial_r T}{T}\right)^2. \tag{13}$$

The container is thus approximated by a sphere of radius L. At the thermodynamic equilibrium the walls are though to be equally preferably wetted by either phase, that is, the Young's angle is $\pi/2$. This condition implies a vanishing normal derivative of the density at the walls [24]

$$\partial_r n|_{r=L} = 0.$$

There is no flow of material through the walls, therefore

$$u|_{r=L} = 0.$$

Boundary conditions at the center of the droplet, $r = 0$, follow from the symmetry argument:

$$u|_{r=0} = \partial_r n|_{r=0} = \partial_r s|_{r=0} = 0.$$

The equations of motion (11) – (13) are then solved numerically using classical finite differences. We use fourth order accurate discrete approximations for the spatial derivatives and third order Runge - Kutta scheme for time-marching [25]. Numerical scheme, similar to one used here, is briefly outlined in Ref. [2]. We used spatial grid consisting of 1024 points for $L = 1024$. We have repeated the computations on the twice finer grid and did not found any significant differences.

III. EVOLUTION OF THERMODYNAMIC QUANTITIES

Initially the system is at thermodynamic equilibrium: the radial velocity, u, is zero everywhere; the temperature of the walls of the container, T_w, is 0.85 (128K for argon); the temperature inside the container is constant $T = T_w$. The initial density profile, shown in Fig.2, corresponds to the vapor bubble with $n = n_v \approx 0.32$ of radius ≈ 134 (669Å for argon) surrounded by the liquid with $n = n_l \approx 1.81$. The radius of the container is $L = \times 1024$ ($\approx 0.51\mu$m for argon). We suddenly rise the temperature of the walls of the container to $T_w = 0.95$ (143.2K for argon) and monitor the evolution of the system towards new equilibrium state, which corresponds to uniform density profile (the initial and the final states are indicated at the phase diagram shown in Fig.1; the final state is in the one-phase region).

The rapid increase of the temperature at the walls excites the wave which moves from the walls towards the bubble (see Figs.3,4). The propagation speed of the wave is close to the velocity of sound in the liquid. When the wave hits the interface it undergoes partial

reflection and excites secondary wave in the vapor phase. It also sets the interface in motion — the bubble shrinks. The temperature of the vapor phase increases and reaches it's maximum value when the (spherical) wave reaches the center of the bubble, $r = 0$. Then the wave gets reflected and propagates back towards the boundaries (see Fig.5). When it reaches the interface from the vapor side, it again undergoes partial reflection. The waves in the liquid phase are also reflected by the walls of the container; resulting interference leads to rather irregular spatial profiles of the thermodynamics quantities. In particular, this irregularity can be seen in the time dependence of the temperature and the density at the center of the bubble, presented in Figs.7,8 respectively. The movie, showing the time evolution of the density and temperature profiles, is available at [26].

The time dependence of the radius of the bubble is given in Fig.9 (the radius of the bubble, R, is defined as the distance from its center to the inflection point at the interface, that is, position where the sign of the second derivative of density changes). The rapid compression of the bubble under the action of the wave is clearly seen in this figure. The overall time dependence of the radius of the condensing bubble is quite different from one observed for the evaporating droplet. The dynamics of the latter process is limited by the heat flow, which leads to the familiar $R^2 \propto t$ law. Here we see something different. Roughly speaking, the radius of the bubble decreases linearly with time: the condensation of a bubble of size 668Å takes $\approx$ 28ns. It is roughly fifty times faster than the evaporation of the same size liquid droplet [3]. Moreover, evaporation, even in sub-micrometer scale, proceeds quasi-stationary [3], whereas condensation does not.

One more interesting point concerns the peak temperature attained at the center of the bubble (see Fig.10). As one can see from that figure, it can reach temperature order of magnitude higher than the temperature at the container walls. It did not escape our

attention that such temperature can promote various reactions inside a bubble or even ionization of elements. The similar mechanism (focusing of the wave energy) is responsible for sonoluminescence [27, 28].

IV. SUMMARY

We have considered the dynamics of iso-volumetric condensation of a spherically symmetric bubble using diffuse interface description. The dynamics has been found to be quite different from that of evaporation. In particular, rather high temperatures (Fig.10) can be attained in the condensing bubble if the process is triggered by rapid change of the container's walls temperature. The time dependence of the radius of the bubble appears to be roughly linear in contrast to the square-root curve observed in the same conditions for the evaporating droplet. The condensation process is hardly quasi-stationary: the bubble disappears before mechanical equilibrium is approached and therefore the motion of the pressure disturbances (waves) is equally important as the heat diffusion. That precludes from using simple approximations which work well for the evaporating droplet.

Acknowledgments

This work has been supported by the KBN grant 2P03B00923 (2002 – 2004).

---

[1] D. Jamet, O. Lebaigue, N. Coutris, and J. M. Delhaye, J.Comp.Phys. **169**, 624 (2001).

[2] V. Babin and R. Hołyst, J.Chem.Phys. **122**, 024713 (2005).

[3] V. Babin and R. Hołyst, J.Phys.Chem.B **to appear** (2005).

[4] J. H. Walther and P. Koumoutsakos, J. Heat Transfer. **123**, 741 (2001).

[5] J. M. Delhaye, Int. J. Multiphase Flow **1**, 395 (1974).

[6] A. Prosperetti and M. S. Plesset, Phys.Fluids **27**, 1590 (1984).

[7] F. J. Higuera, Phys.Fluids **30**, 679 (1987).

[8] D. Bedeaux, L. J. F. Hermans, and T. Ytrehus, Physica A **169**, 263 (1990).

[9] G. Fang and C. A. Ward, Phys.Rev.E **59**, 417 (1998).

[10] T. Ytrehus and S. Østmo, Int.J.Multiphase Flow **22**, 133 (1996).

[11] L. A. Turski and J. S. Langer, Phys.Rev.A **22**, 2189 (1980).

[12] R. Venugopalan and A. P. Vischer, Phys.Rev.E **49**, 5849 (1994).

[13] B. U. Felderhof, Physica **48**, 541 (1970).

[14] J. S. Langer and L. A. Turski, Phys.Rev.A **8**, 3230 (1973).

[15] D. M. Anderson and G. B. McFadden, Internal Report 5887, National Institute of Standards and Technology (1996).

[16] L. K. Antanovskii, Phys.Rev.E **54**, 6285 (1996).

[17] J. S. Rowlinson and B. Widom, *Molecular Theory of Capillarity* (Oxford University Press, Oxford, 1989).

[18] P. C. Hohenberg and B. I. Halperin, Rev.Mod.Phys. **49**, 435 (1977).

[19] L. D. Landau and E. M. Lifshiz, *Fluid Mechanics* (Pergamon Press, Oxford, 1987).

[20] D. M. Anderson, G. B. McFadden, and A. A. Wheeler, Ann.Rev.Fluid Mech. **30**, 139 (1998).

[21] P. Español, J.Chem.Phys. **115**, 5392 (2001).

[22] L. D. Landau and E. M. Lifshiz, *Statistical Physics, Part.1* (Pergamon Press, Oxford, 1980).

[23] `http://webbook.nist.gov/chemistry/fluid/`.

[24] P. Seppecher, Int.J.Eng.Sci **34**, 977 (1996).

[25] C. W. Shu and S. Osher, J.Comp.Phys. **77**, 439 (1988).

[26] *The movie which shows time evolution of the density and temperature profiles*, `http://www.ichf.edu.pl/diffuse-interface/condensation.avi`.

[27] D. Lohse, Nature **434**, 33 (2005).

[28] D. J. Flannigan and K. S. Suslick, Nature **434**, 52 (2005).

Figures

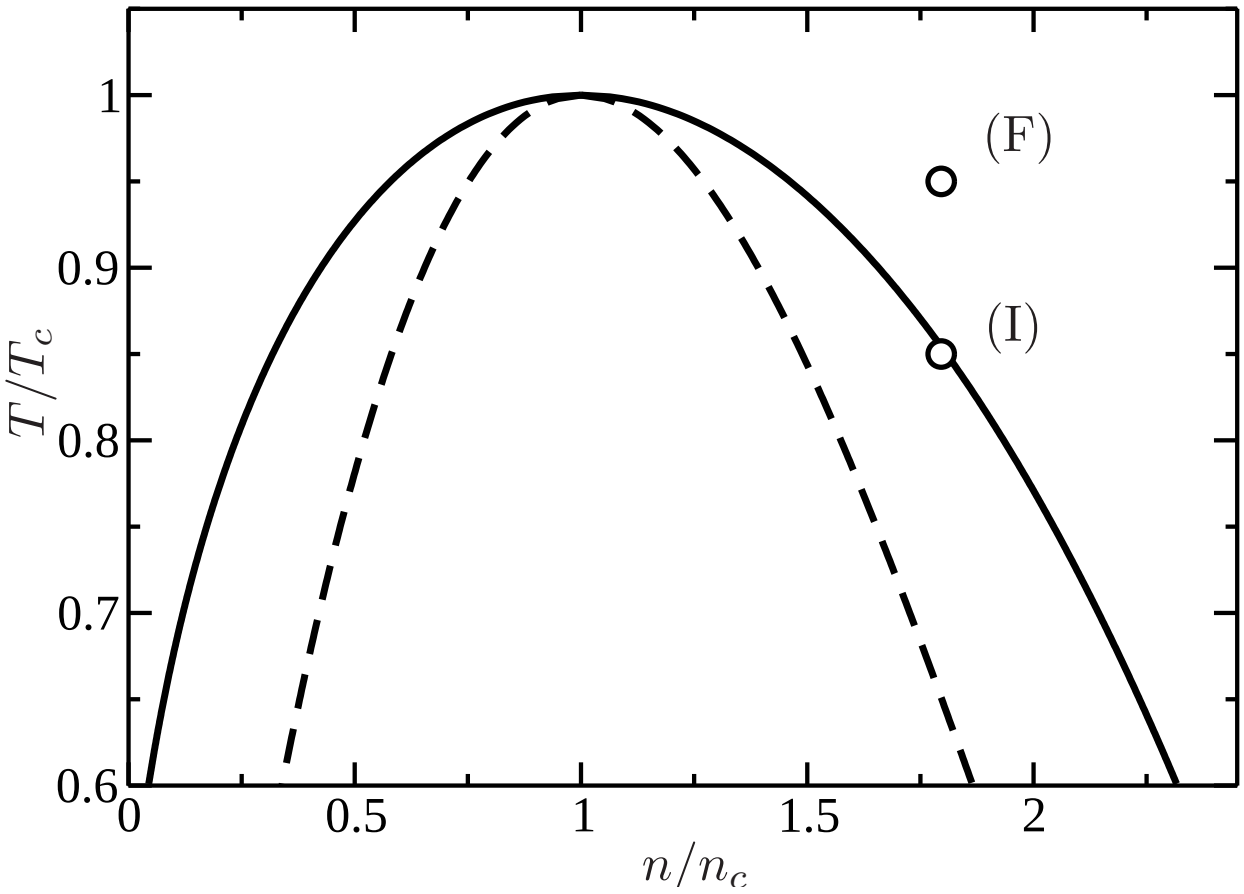

FIG. 1: The phase diagram of the liquid/vapor system described by by the bulk free energy density (7). The solid line represents the liquid/vapor coexistence line, that is, the line where for given density, n, and temperature, T, the pressures and the chemical potential in both phases are equal. The dashed line represents the spinodal, that is, the line where isothermal compressibility of the substance diverges. The initial (I) and the final (F) states of the simulation are also shown.

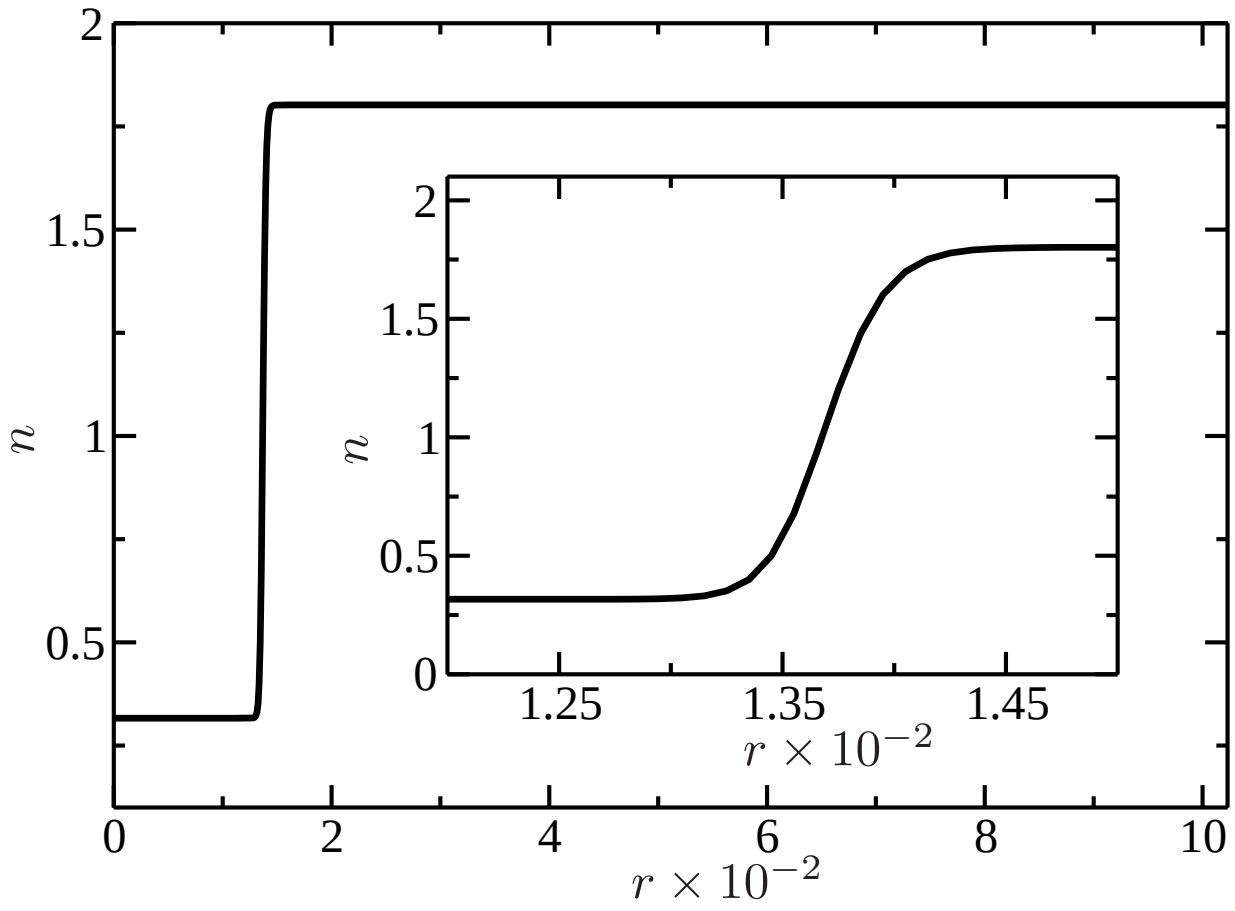

FIG. 2: Initial density profile. The density, n, is in units of the critical density; the radial coordinate, r, is in units of δ_L (for argon $\delta_L = 4.99 \times 10^{-10} m$).

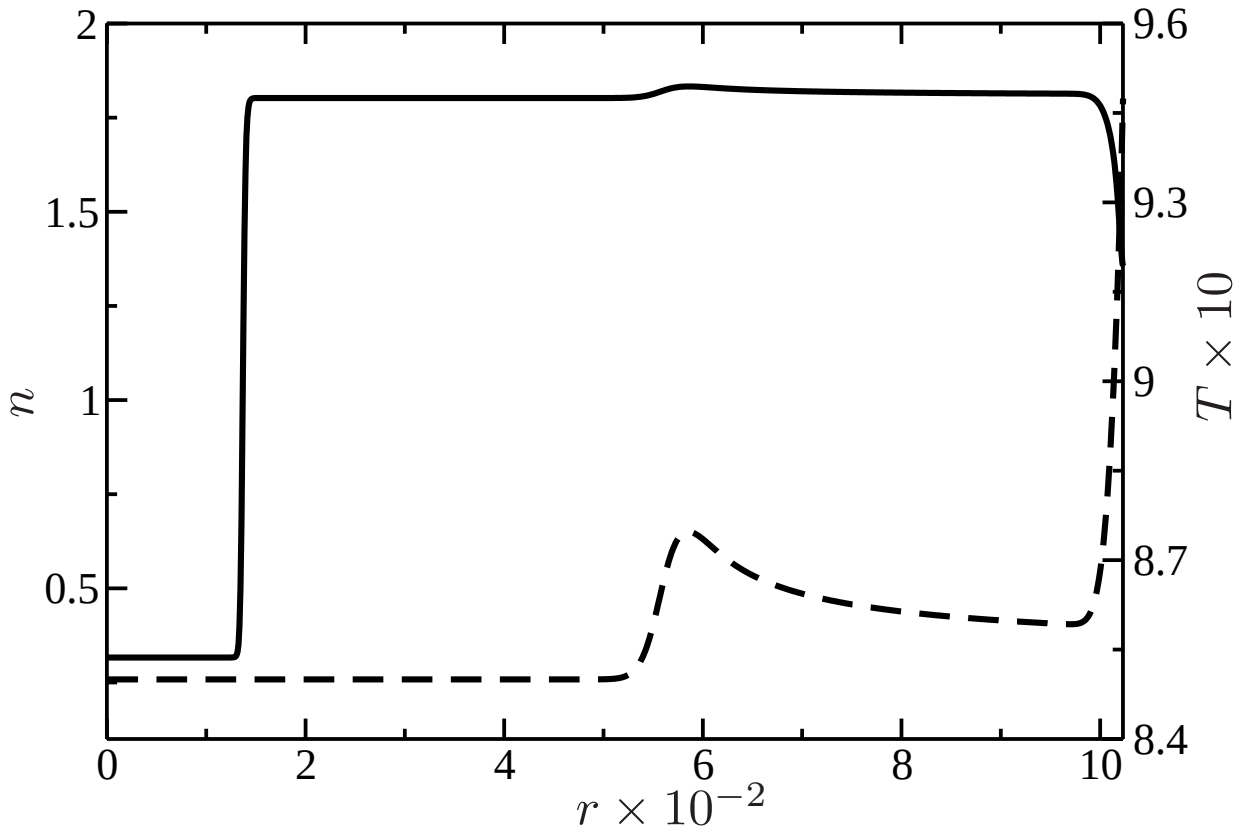

FIG. 3: Profiles of the density (solid line), n, and the temperature (dashed line), T, at time $t = 200$ after the temperature of the container's walls, T_w, was raised. The density, n, and the temperature, T, are in units of the critical density and temperature respectively. The radial coordinate, r, and the time t are in units of δ_L and δ_t respectively (for argon $\delta_L = 4.99 \times 10^{-10} m$ and $\delta_t = 2.82 \times 10^{-12} s$).

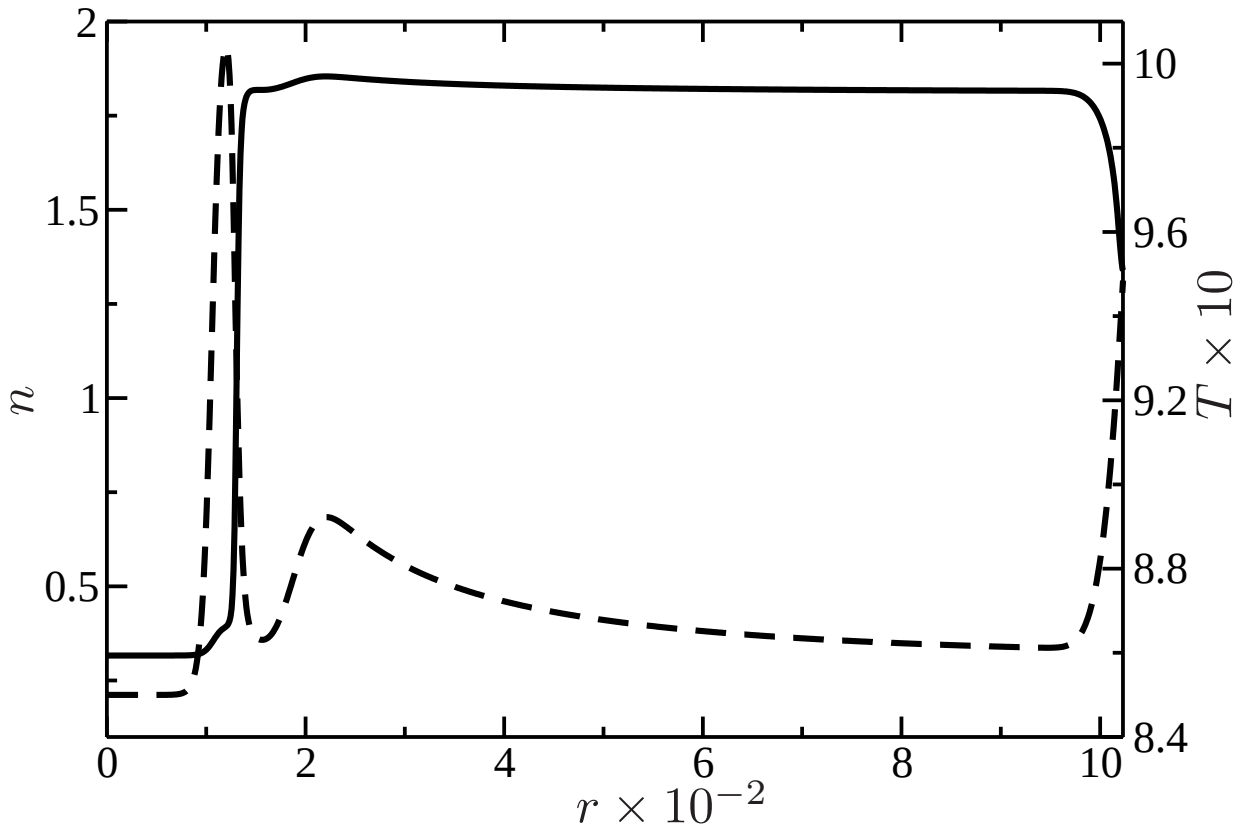

FIG. 4: Profiles of the density (solid line), n, and the temperature (dashed line), T, at time $t = 400$ after the temperature of the container's walls, T_w, was raised. The units are the same as in Fig. 3.

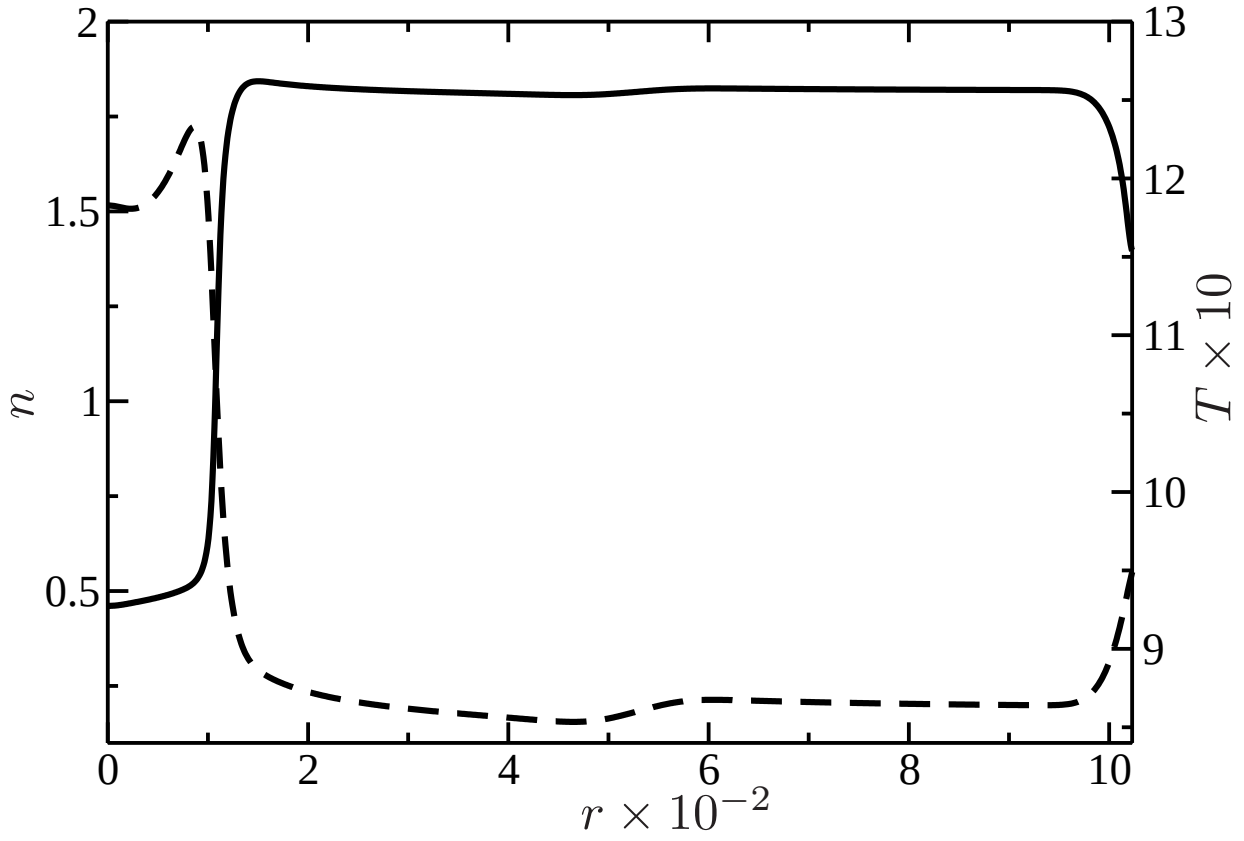

FIG. 5: Profiles of the density (solid line), n, and the temperature (dashed line), T, at time $t = 550$ after the temperature of the container's walls, T_w, was raised. The units are the same as in Fig. 3.

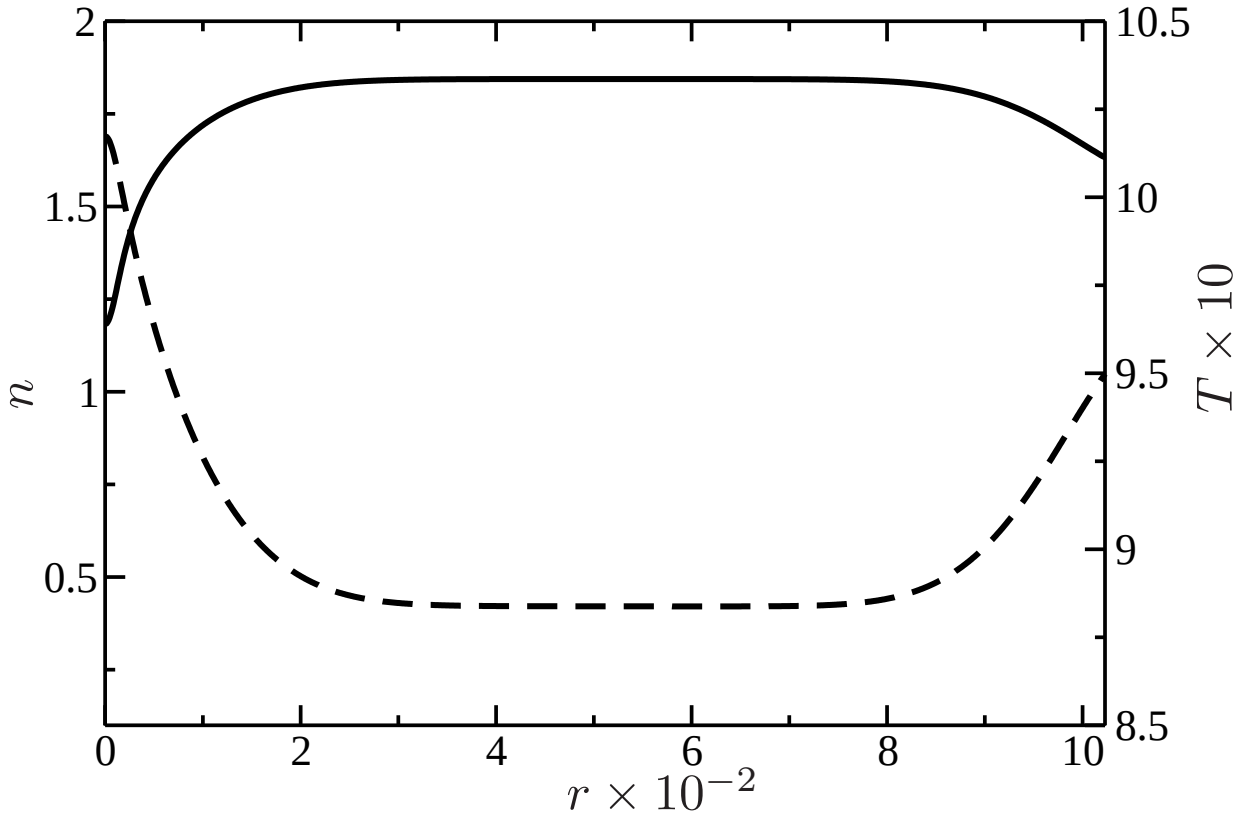

FIG. 6: Profiles of the density (solid line), n, and the temperature (dashed line), T, at time $t = 8000$ after the temperature of the container's walls, T_w, was raised. The units are the same as in Fig. 3.

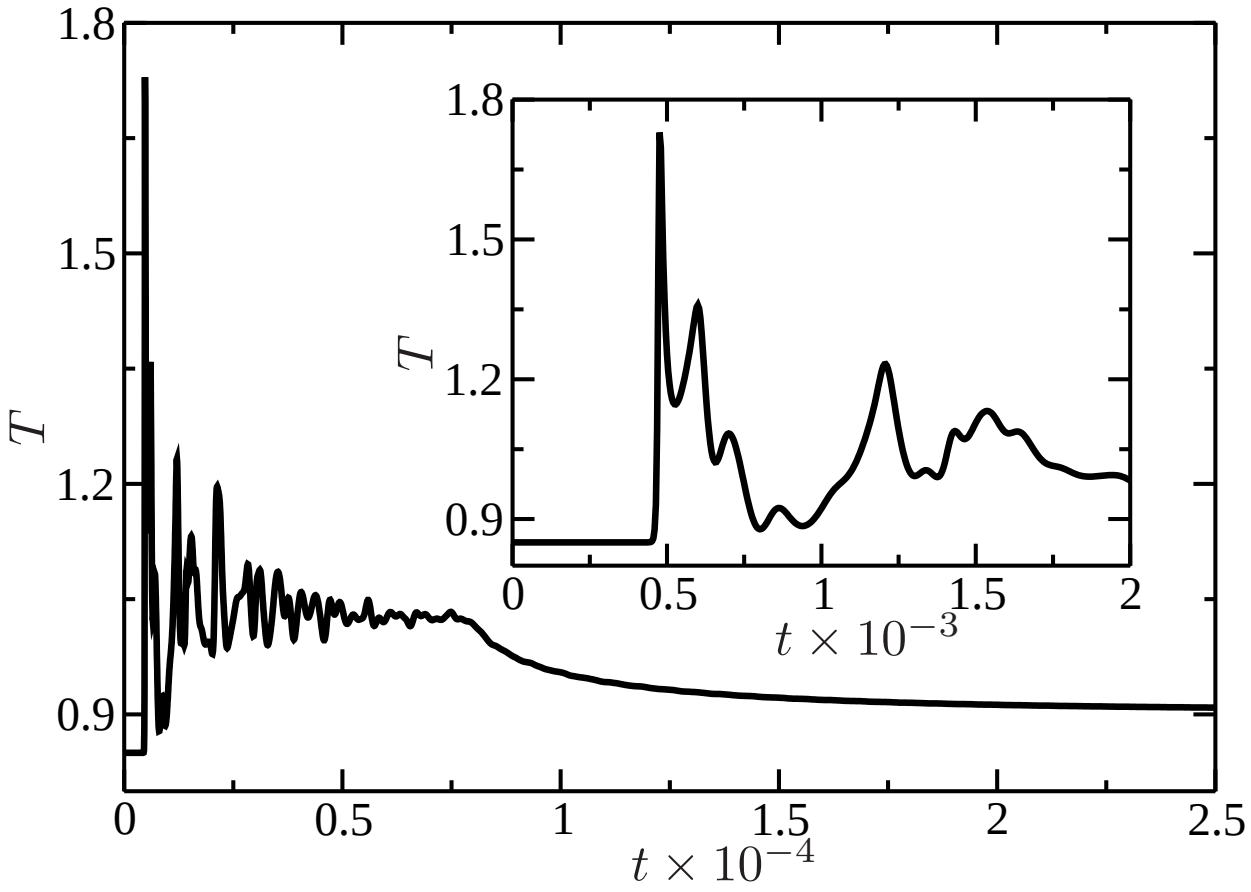

FIG. 7: The temperature, T, at the center of the bubble, $r = 0$, as a function of time after the wall's temperature has been raised. The temperature is in units of critical temperature and the time, t, is in units of δ_t (for argon $\delta_t = 2.82 \times 10^{-12} s$).

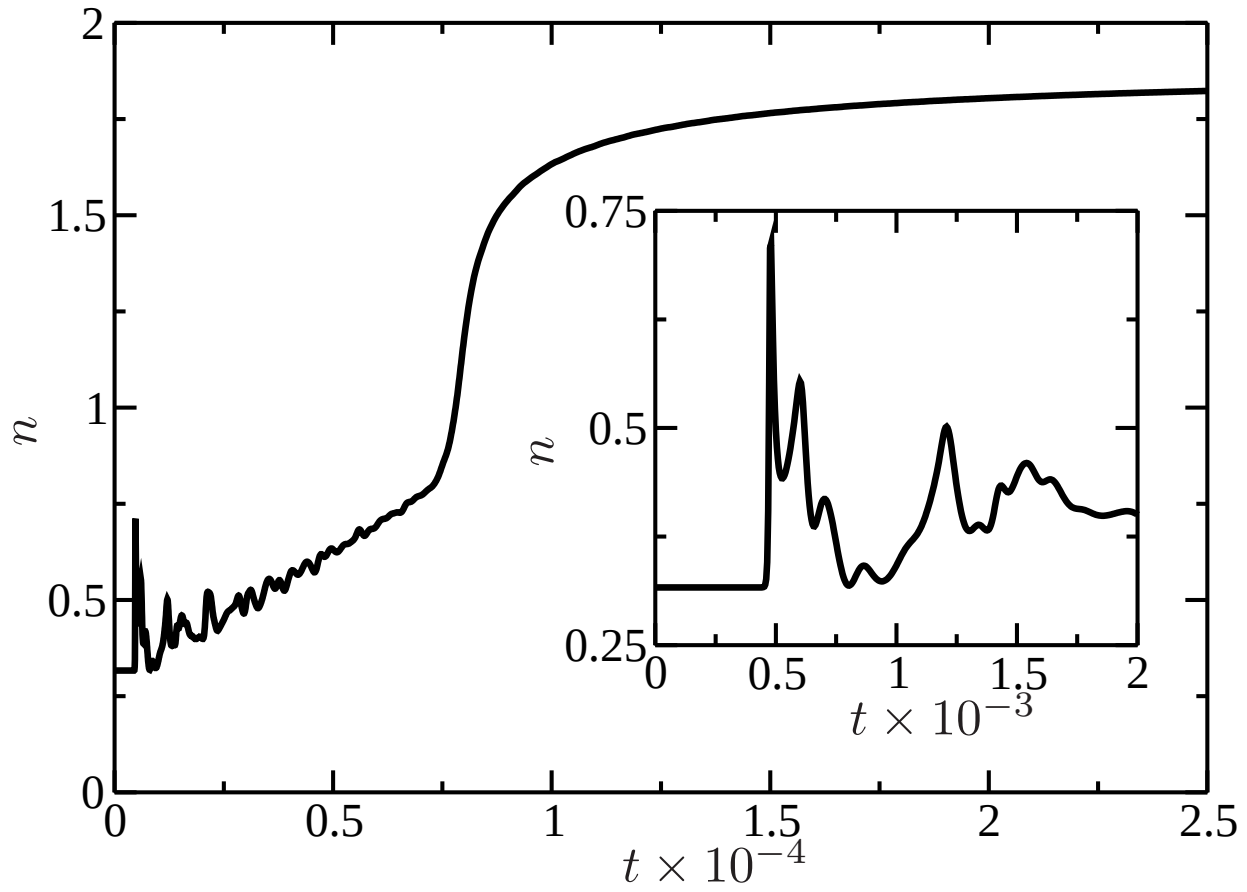

FIG. 8: The density, n, at the center of the bubble, $r = 0$, as a function of time after the wall's temperature has been raised. The density is in units of critical density and the time, t, is in units of δ_t (for argon $\delta_t = 2.82 \times 10^{-12} s$). Practically the process of condensation is complete after $t \approx 10^4$ time steps ($\approx$ 28ns for argon).

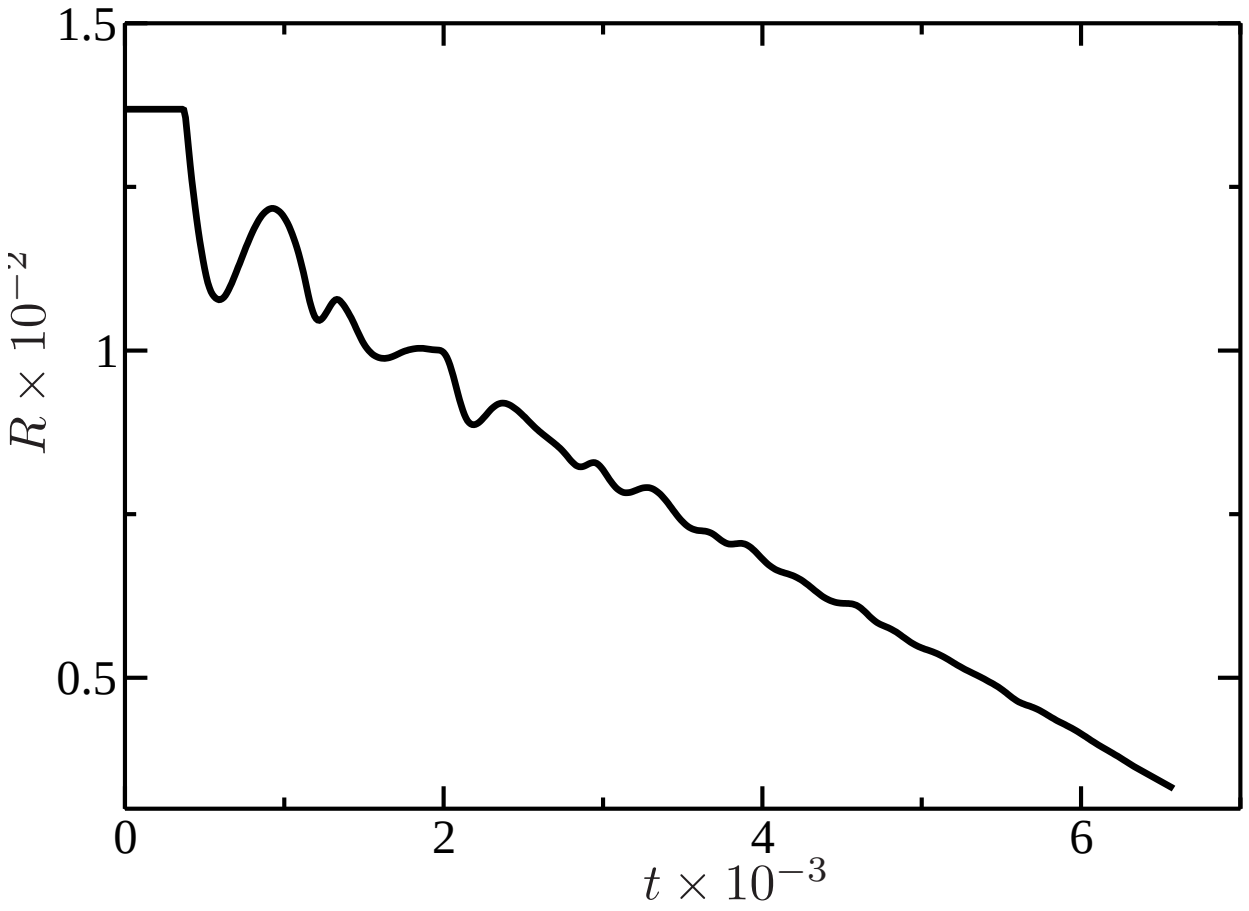

FIG. 9: Time dependence of the bubble radius, R. The radius is in units of δ_L and the time, t, is units of δ_t (for argon $\delta_L = 4.99 \times 10^{-10} m$ and $\delta_t = 2.82 \times 10^{-12} s$). The radius decreases roughly linearly with time (after $t \approx 6500$ the profile looses its inflection point for $r > 0$ and the radius becomes undefined).

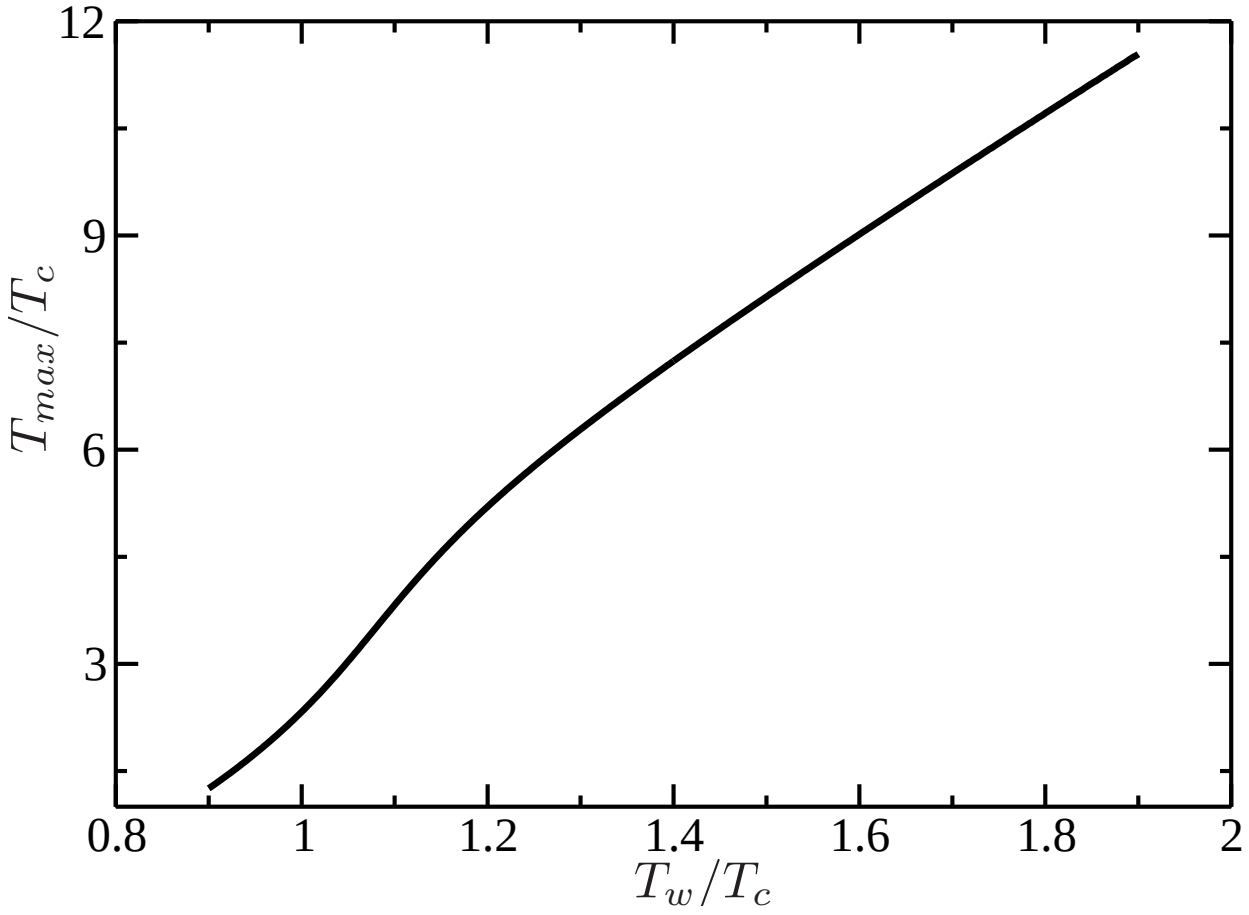

FIG. 10: Highest temperature, T_{max}, attained inside the bubble as a function of the wall's temperature T_w (in units of the critical temperature T_c). For argon ($T_c = 150.6$K) the increase of walls temperature to 240K induces a maximal temperature ≈ 1356K inside the bubble.